hep-ph/9406395
June 1994

FOUR WEAK BOSON PRODUCTION IN TEV PHOTON–PHOTON COLLISIONS AND HEAVY HIGGS SIGNAL[1]

G. Jikia

Institute for High Energy Physics
142284, Protvino, Moscow region, Russia

Abstract

We study the signals for a heavy Higgs boson in the processes $\gamma\gamma \to WWWW$, $\gamma\gamma \to WWZZ$ at the photon linear collider. The results are based on the first complete tree level calculation for these reactions. Using a forward "spectator" W tag, central "spectator" W veto to suppress backgrounds from transverse W, Z production we show that the invariant mass spectrum of central WW, ZZ pairs is sensitive to Higgs boson with a mass up to 1 TeV at a 2 TeV linear collider.

1 Introduction

One of the most challenging puzzles of contemporary particle physics is whether Nature indeed makes use of the Higgs mechanism of spontaneous electroweak symmetry breaking. If Higgs boson will be found below 800 GeV or so, this will be a proof of the so called weak scenario of the symmetry breaking. Otherwise the scenario of the strongly interacting electroweak sector (SEWS) will take place (for recent reviews see *e.g.* [1]). The study of SEWS is one of the major motivations to built the next generation of colliders. While the potential of hadronic colliders (see *e.g.* [2] and references therein) as well as linear e^+e^- colliders [3] to explore SEWS was extensively studied, much less was done for $\gamma\gamma$ colliders [4], which are the main subject of this Workshop.

The would be "gold-plated" channel for Higgs boson production at a $\gamma\gamma$ collider

$$\gamma\gamma \to H \to ZZ \to (q\bar{q})(l^+l^-) \tag{1}$$

was shown recently to be suffered from very large background from continuum ZZ pair production through W boson loop for the Higgs mass above 350 GeV [5]. So

[1]Based on invited talk given at the *"Workshop on gamma–gamma colliders"*, March 28-31, 1994, Lawrence Berkeley Laboratory

this reaction, although very promising for the measurement of the two-photon Higgs width for $M_H \leq 300 - 400$ GeV, provides very poor possibilities for studying of a heavy Higgs and SEWS (see also [6]).

Another very interesting potential application of photon-photon collisions at a high energy linear collider proposed recently [7] is WW scattering, as illustrated in Fig. 1. In this process each photon is resolved as a WW pair. The interacting vector bosons can then scatter pair-wise or annihilate; *e.g.* they can annihilate into a Higgs boson decaying into a WW or ZZ pair. In principle, one can use these processes

$$\gamma\gamma \to W^+W^+W^-W^-, \quad W^+W^-ZZ \tag{2}$$

for studying SEWS. In fact this reaction at photon-photon collider is an analog of the reaction $e^+e^- \to \nu\bar{\nu}WW(\nu\bar{\nu}ZZ)$ at linear e^+e^- collider. Event rates for the reaction (2) were estimated using effective W approximation (EWA) [8] for several models of SEWS and quite optimistic conclusions were given. However, EWA has a limited accuracy at energies of 1-2 TeV and, moreover, it does not permit to calculate the effects of the tag and veto cuts used to isolate the Higgs signal (*e.g.* K. Cheung [8] had to use the exact calculation for the reaction $\gamma\gamma \to WWH$ to estimate the efficiencies of these cuts).

In this paper we present results of the exact standard model tree level calculation for the reactions (2). In Section 2 we present cross sections for different polarizations of $WWWW$, $WWZZ$ final states. In Section 3 we show that Higgs boson with a mass up to 700 GeV should be relatively easily observed in photon-photon collisions at a 1.5 TeV linear collider. Then we will concentrate on the heavy ($m_H = 1$ TeV) standard model Higgs boson case as a prototype for models of SEWS and will show that its signal can be observed at a 2 TeV linear collider. We conclude with some brief remarks in Section 4.

2 Cross sections

Total cross sections for the processes of four gauge boson production in $\gamma\gamma$ collisions as a function of c.m. energy are shown in Fig. 2. For comparison also are shown cross sections for other typical reactions in e^+e^- and $\gamma\gamma$ collisions (from [9]). One notes that four weak boson $WWWW(WWZZ)$ production in $\gamma\gamma$ collisions is larger than $\nu\bar{\nu}WW(\nu\bar{\nu}ZZ)$ production in e^+e^- collisions at the same energy. Of course, this does not mean that the Higgs boson signal is larger in photon-photon collisions, as both cross sections are dominated by transverse gauge boson contributions.

Cross sections for different initial and final polarization states and two values of the Higgs mass $m_H = 100$ GeV and $m_H = \infty$ are shown in Fig. 3 for four W boson production. One can see that the cross sections are slightly larger for equal initial photon helicities. The dominating contributions come from the production of all four gauge bosons being transverse and one longitudinal and the other three

transverse W's. The ratio of $TTTT/TTTL$ is about $(60 \div 70)\%$. Such large fraction of $TTTL$ polarization state is due to production of soft W_L and the analogous effect was observed earlier for $\gamma\gamma \to WWZ$ reaction [9]. The contributions from two longitudinal weak bosons $TTLL$ and $TLTL$ are about an order of magnitude smaller than that for $TTTT$ production. The yield of $TLLL$ and $LLLL$ final states is even smaller, however one can see that for infinite Higgs boson mass their contribution can be orders of magnitude larger than for a 100 GeV Higgs. It is this rise of the cross section of longitudinal electro-weak boson interactions that signals SEWS [1]. This effect is illustrated in Fig. 4 where cross sections of $TTTT + TTTL$ as well as of final states containing at least two longitudinal gauge bosons production are compared for $m_H = 100$ GeV and $m_H = \infty$. As usual, we can define the heavy Higgs boson signal to be the difference between the cross section with a heavy Higgs boson and the result with a light Higgs boson, *e.g.*

$$\sigma(\text{signal for } m_H = \infty) = \sigma(m_H = \infty) - \sigma(m_H = 100 \text{ GeV}). \tag{3}$$

Consequently, cross section for light Higgs boson represents the background. From Fig. 4 one can conclude that signal-to-background ratio is about 10% for total cross sections.

3 Signal of heavy Higgs boson at photon linear collider

The scattering reaction (2) leads to two scattered W's or Z's emerging at large transverse momentum in the final state accompanied by two "spectator" W's at low $p_\perp$ focussed along the beam direction. And the heavy Higgs signal can be observed in the invariant mass spectrum of the two hard scattered weak bosons. To select these W's or Z's we number all the final gauge bosons according to their angles θ_i with beam direction:

$$|\cos\theta_1| > |\cos\theta_2| > |\cos\theta_3| > |\cos\theta_4|. \tag{4}$$

We are interested in the mass spectrum of the "central" pair $m(V_3V_4)$, where V denotes W or Z and we also assume that hadronic decay modes of the central pair will be observed, *i.e.* we will not distinguish W's from Z's. The crucial point to note is that in the framework of EWA the initial W_L's participating in the W_LW_L scattering have a $1/(p_\perp^2 + M_W^2)^2$ distribution with respect to initial photons from which they are produced. This is to be contrasted with a $p_\perp^2/(p_\perp^2 + M_W^2)^2$ distribution of the initiating W_T's, leading *e.g.* to W_TW_T scattering. Analogous effect is known to take place for W distribution in quark – (anti-) quark or e^+e^- collisions [1, 2]. The softer $p_\perp$ distribution in the W_LW_L case has an important consequence: the spectator W's tend to emerge with smaller $p_\perp$ and correspondingly smaller angle than those associated with the background processes of W_TW_T or W_TW_L scattering. Therefore

we will divide four final gauge bosons in two pairs of forward (backward) V_1V_2 and central V_3V_4 according to ordering (4) and will impose different cuts on these pairs. We will veto hard forward (backward) W's $|\cos\theta_{1,2}| < z_f$ and will also require that $|\cos\theta_{3,4}| > z_c$ to enhance the signal/background ratio. Although it is the invariant mass $m(V_3V_4)$ which we are interested in, to separate four gauge boson production from backgrounds which come from $\gamma\gamma \to W^+W^-$ and $\gamma\gamma \to W^+W^-Z$ reactions we will also tag forward (backward) spectators $V_{1,2}$ in the region outside the dead cone along the beam direction $|\cos\theta_{1\div4}| < z_0$, where z_0 is determined by the acceptance of experimental installation. The experimental signature is then given by four hard jets from $WW(ZZ)$ decay in the central region with a branching ratio of 50% and jets or leptons in forward and backward regions from the decay of spectator W's. We have not modelled W, Z decays, so cuts will be imposed on momenta of vector bosons.

In Tables 1 and 2 we summarize cross sections and selection efficiencies for a set of cuts for $WWWW$, $WWZZ$ production at photon-photon collider realized at 1.5 and 2 TeV linear collider taking into account photon luminosity spectrum [4]. Cross sections are quite large, for example about ten thousand events of four weak boson production will be observed at 2 TeV linear collider with $\int \mathcal{L}dt = 200$ fb^{-1}. It is important to note that increasing dead cone from 5° to 10° we are loosing a large fraction of the signal events.

In Figures 5, 6, we present the invariant mass distribution of the central WW, ZZ pairs summed over $WWWW$ and $WWZZ$ final states for two different cuts and c.m. energies of 1.5 and 2 TeV. The number of events corresponds to integrated luminosity of 200 fb^{-1}. First, at 1.5 TeV we see clear peaks from the Higgs resonance at 500 and 700 GeV. Thus, in principle one can observe a Higgs boson heavier than 350 GeV at the photon-photon collider. However these events emerge from WW fusion and have nothing to do with the two-photon Higgs width measurements. Also, it is hardly possible to push the observable Higgs mass well above 700 GeV at 1.5 TeV machine. Secondly, at a 2 TeV linear collider one can observe a signal from 1 TeV Higgs boson. For a dead cone of 5° one can see a very distinctive enhancement around the invariant mass of 1 TeV. For $z_0 = \cos(10°)$ the signal is still statistically significant, although not so pronounced. For the infinitely heavy Higgs boson the invariant mass spectrum is almost structureless at 2 TeV and more energy is needed to observe the picture analogous to that in Fig. 6. Event rates as well as signal/background ratio and the statistical significance corresponding to Figs. 5, 6 are given in Table 3. Comparing this table with Tables 1, 2 we see that while the signal contributes only about 10% to the total cross section for $m_H = 1$ TeV, appropriate cuts permit to enhance the signal-to-background ratio by an order of magnitude.

4 Discussion

The most important question is, certainly, comparison of the potential of photon-photon collider with that of other machines. For hadronic and e^+e^- colliders much

more detailed investigations were done including decays of final W's and Z's and detector simulations [1–3]. For example, conclusion was done [3] that the signal from 1 TeV Higgs boson was distinguishable from the case of massless Higgs at the c.m. energy of e^+e^- collider of 1.5 TeV and integrated luminosity of 200 fb^{-1}. However, it was also found that the integrated luminosity of 310 fb^{-1} and 80 fb^{-1} were needed to discriminate the $m_H = \infty$ signal at 3σ level at 2 TeV and 3 TeV linear collider, respectively. So, we can very roughly estimate that potential of 2 TeV linear collider in photon-photon mode is the same as that of 1.5 TeV e^+e^- collider, provided that their luminosities are the same. But what we would like to stress, is that because of different conditions at the interaction point luminosity of high energy photon-photon collider has a much less restrictive upper bound than that for e^+e^- collider [4]. And it is even stated that such a huge luminosity as 10^{35-36} cm^{-2} s^{-1} is technically achievable in photon-photon collisions [4]. Therefore, if such a luminosity will be really achieved and if it will be possible to make experiments at such a huge luminosity, photon-photon option will become very competitive with normal e^+e^- mode of linear collider.

Acknowledgements

I am grateful to M. Berger, F. Boudjema, S. Brodsky, K. Cheung, I. Ginzburg, T. Han, F. Richard, V. Serbo and V. Telnov for helpful discussions. I am indebted to G. Bélanger for making available the figures for $\gamma\gamma$ and e^+e^- processes. Special thanks to organizers of the Workshop for financial help and to A. Sessler and M. Chanowitz for kind hospitality. The attendance at the Workshop was supported, in part, by the International Science Foundation travel grant.

References

[1] M.S. Chanowitz, in Proc. of the *2-nd KEK Topical Conference on e^+e^- Collision Physics*, Tsukuba, Japan, November 26-29, 1991; K.-I. Hikasa, in Physics and Experiments with Linear e^+e^- Colliders, Saariselkä, Finland, 1992, Ed. R. Orava *et al.*, World Scientific, p. 451; T. Han, in Physics and Experiments with Linear e^+e^- Colliders, Waikoloa, Hawaii, 1993, Ed. F.A. Harris *et al.*, World Scientific, vol. I, p. 270.

[2] J. Bagger, V. Barger, K. Cheung, J. Gunion, T. Han, G.A. Ladinsky, R. Rosenfeld, and C.P. Yuan, *Phys. Rev.* **D49** (1994) 1246.

[3] K. Hagiwara, J. Kanzaki, and H. Murayama, KEK Report No. 91-4 (March 1991); Y. Kurihara, R. Najima, *Phys. Lett.* **B301** (1993) 292; Y. Kurihara, R. Najima, KEK-Preprint-93-90, August 1993.

[4] V.E. Balakin, these proceedings; V.I. Telnov, these proceedings and in Physics and Experiments with Linear e^+e^- Colliders, Waikoloa, Hawaii, 1993, Ed. F.A. Harris *et al.*, World Scientific, vol. II, p. 551.

[5] G.V. Jikia, *Phys. Lett.* **298B** (1993) 224, *Nucl. Phys.* **B405** (1993) 24; B. Bajc, *Phys. Rev.* **D48** (1993) 1907; M.S. Berger, *Phys. Rev.* **D48** (1993) 5121; D.A. Dicus, C. Kao, *Phys. Rev.* **D49** (1994) 1265; H. Veltman, report SACLAY-SPHT-93-111, October 1993.

[6] M.S. Berger, these proceedings.

[7] S. Brodsky, in Physics and Experiments with Linear e^+e^- Colliders, Waikoloa, Hawaii, 1993, Ed. F.A. Harris *et al.*, World Scientific, vol. I, p. 295.

[8] K. Cheung, *Phys. Lett.* **B323** (1994) 85, and these proceedings.

[9] M. Baillargeon, F. Boudjema, *Phys. Lett.* **B317** (1993) 371; M. Baillargeon, G. Belanger, and F. Boudjema, ENSLAPP-A-473-94, May 1994.

Figure captions

Fig. 1. WW scattering at a photon-photon collider.

Fig. 2. Typical cross sections of electroweak reactions at $\gamma\gamma$ and e^+e^- modes of linear collider. For $t\bar{t}$ production the top mass was set to 130 GeV. The other subscripts refer to the mass of the Higgs. For reactions $e^+e^- \to WW\nu\bar{\nu}, ZZ\nu\bar{\nu}$ Higgs mass was set to zero.

Fig. 3. Cross sections for different polarization states of initial and final particles of the reaction $\gamma\gamma \to W^+W^+W^-W^-$ for $m_H = 100$ GeV and $m_H = \infty$ as a function of $\gamma\gamma$ c.m. energy. $TTLL$ ($TLTL$) curves correspond to final states with W_TW_T and W_LW_L pairs of the same- (opposite-) charges.

Fig. 4. Comparison between the cross sections for $m_H = 100$ GeV and $m_H = \infty$ for equal and opposite helicities of the initial photons. For the reaction $\gamma\gamma \to WWWW$ solid line is the total cross section; dotted line is the $TTTT + TTTL$ cross section; dashed line is the sum of cross sections with at least two longitudinal final W's. For the reaction $\gamma\gamma \to WWZZ$ corresponding cross sections are denoted by solid, dotted and dash-dotted lines.

Fig. 5. Event rates for $WWWW + WWZZ$ production in $\gamma\gamma$ collisions at 1.5 TeV linear collider for $m_H = 100$ (shaded histogram), 500 and 700 GeV (hatched histogram) for different cuts.

Fig. 6. Event rates for $WWWW + WWZZ$ production in $\gamma\gamma$ collisions at 2 TeV linear collider for $m_H = 100$ (shaded histogram) and 1000 GeV for different cuts.

Table captions

Table 1: Cross sections (in fb) and selection efficiencies for $\gamma\gamma \to W^+W^+W^-W^-$ and $\gamma\gamma \to W^+W^-ZZ$ for $m_H = 100$ GeV, 1 TeV and ∞ at $\sqrt{s_{e^+e^-}} = 1.5$ TeV including various cuts. 1) no cut; 2) $|\cos\theta_{1,2}| > 0.9$, $|\cos\theta_{3,4}| < 0.7$; 3) $|\cos\theta_{1\div4}| < \cos(10^\circ)$, $|\cos\theta_{1,2}| > 0.9$, $|\cos\theta_{3,4}| < 0.7$; 4) $|\cos\theta_{1\div4}| < \cos(5^\circ)$, $|\cos\theta_{1,2}| > 0.9$, $|\cos\theta_{3,4}| < 0.7$; 5) $|\cos\theta_{1\div4}| < \cos(5^\circ)$; 6) $|\cos\theta_{1\div4}| < \cos(10^\circ)$.

Table 2: The same as Table 1 but for $\sqrt{s_{e^+e^-}} = 2$ TeV and slightly different cuts. 1) no cut; 2) $|\cos\theta_{1,2}| > 0.95$, $|\cos\theta_{3,4}| < 0.7$; 3) $|\cos\theta_{1\div4}| < \cos(10^\circ)$, $|\cos\theta_{1,2}| > 0.95$, $|\cos\theta_{3,4}| < 0.7$; 4) $|\cos\theta_{1\div4}| < \cos(5^\circ)$, $|\cos\theta_{1,2}| > 0.95$, $|\cos\theta_{3,4}| < 0.7$; 5) $|\cos\theta_{1\div4}| < \cos(5^\circ)$; 6) $|\cos\theta_{1\div4}| < \cos(10^\circ)$.

Table 3: Event rates for signal (S) and background (B) summed over $WWWW$ and $WWZZ$ final states as well as signal/background ratio and the number of standard deviations for two values of the dead cone angle. Cuts correspond to those of Figs. 5, 6. The value of integrated luminosity of 200 fb^{-1} is assumed and branching ratio of 50% for hadronic decays of WW, ZZ pairs is included. At $\sqrt{s} = 1.5$ TeV we require that the invariant mass M_{34} of central pair lie in the interval 400 GeV$< M_{34} <$ 600 GeV for $m_H = 500$ GeV and 500 GeV$< M_{34} <$ 800 GeV for $m_H = 700$ GeV. For $m_H = 1$ TeV and $\sqrt{s} = 2$ TeV 450 GeV$< M_{34} <$ 1.1 TeV.

$\sqrt{s_{e^+e^-}} = 1.5$ TeV						
	$\gamma\gamma \to W^+W^+W^-W^-$			$\gamma\gamma \to W^+W^-ZZ$		
m_H	100 GeV	1 TeV	∞	100 GeV	1 TeV	∞
1	30.6 fb	32.7 fb	32.3 fb	6.85 fb	7.91 fb	7.58 fb
2	2.94 (10%)	3.39 (10%)	3.29 (10%)	.632 (9%)	.870 (11%)	.789 (10%)
3	1.52 (5%)	1.64 (5%)	1.63 (5%)	.331 (5%)	.404 (5%)	.376 (5%)
4	2.63 (9%)	2.96 (9%)	2.87 (9%)	.566 (8%)	.750 (9%)	.684 (9%)
5	28.3 (93%)	29.9 (91%)	29.6 (92%)	6.46 (94%)	7.31 (92%)	7.02 (93%)
6	20.8 (68%)	21.5 (66%)	21.3 (66%)	5.07 (74%)	5.54 (70%)	5.38 (71%)

Table 1:

$\sqrt{s_{e^+e^-}} = 2$ TeV						
	$\gamma\gamma \to W^+W^+W^-W^-$			$\gamma\gamma \to W^+W^-ZZ$		
m_H	100 GeV	1 TeV	∞	100 GeV	1 TeV	∞
1	61.1 fb	68.1 fb	65.6 fb	14.3 fb	17.9 fb	16.1 fb
2	3.10 (5%)	4.01 (6%)	3.67 (6%)	.701 (5%)	1.31 (7%)	1.01 (6%)
3	.691 (1%)	.805 (1%)	.791 (1%)	.161 (1%)	.238 (1%)	.187 (1%)
4	2.46 (4%)	2.99 (4%)	2.74 (4%)	.554 (4%)	.909 (5%)	.731 (5%)
5	53.7 (88%)	58.4 (86%)	56.5 (86%)	12.9 (90%)	15.5 (86%)	14.2 (88%)
6	33.6 (55%)	35.6 (52%)	34.5 (53%)	8.95 (63%)	10.1 (57%)	9.52 (59%)

Table 2:

		$z_0 = \cos(10^\circ)$				$z_0 = \cos(5^\circ)$			
$\sqrt{s_{e^+e^-}}$, TeV	m_H, GeV	S	B	S/B	$S/\sqrt{B}$	S	B	S/B	$S/\sqrt{B}$
1.5	500	84	34	2.5	14	218	56	3.9	29
	700	24	23	1.0	5.0	53	37	1.4	8.7
2	1000	14	21	0.67	3.0	74	59	1.3	9.6

Table 3:

This figure "fig1-1.png" is available in "png" format from:

http://arXiv.org/ps/hep-ph/9406395v1

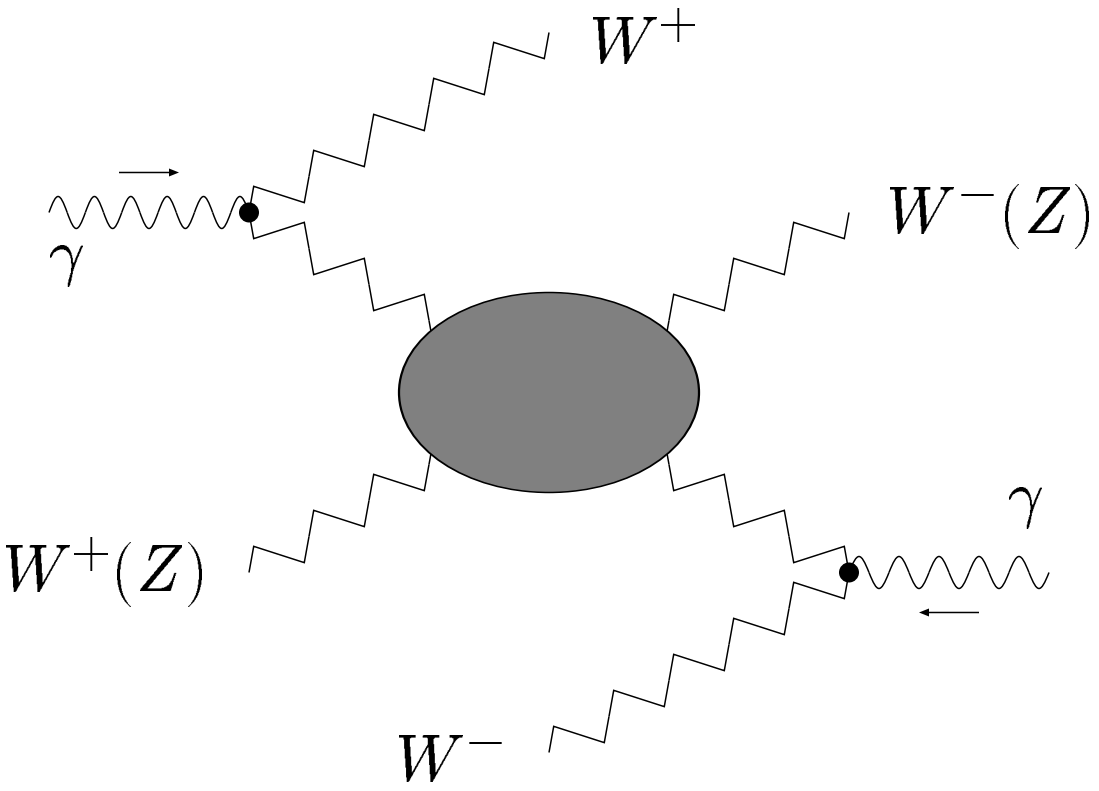

Figure 1. G. Jikia: Four weak boson production ...

This figure "fig1-2.png" is available in "png" format from:

http://arXiv.org/ps/hep-ph/9406395v1

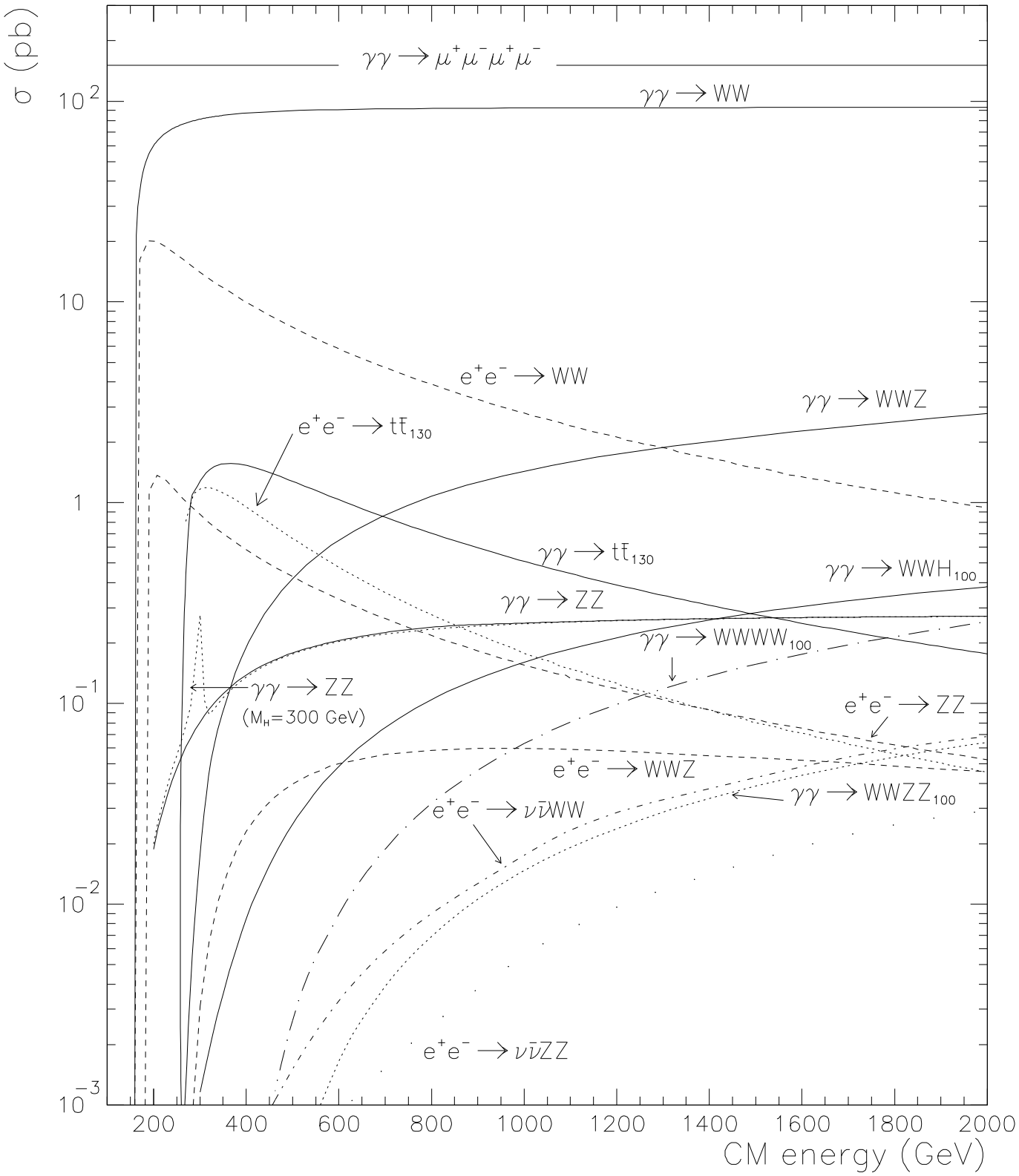

Figure 2. G. Jikia, Four weak boson production ...

This figure "fig1-3.png" is available in "png" format from:

http://arXiv.org/ps/hep-ph/9406395v1

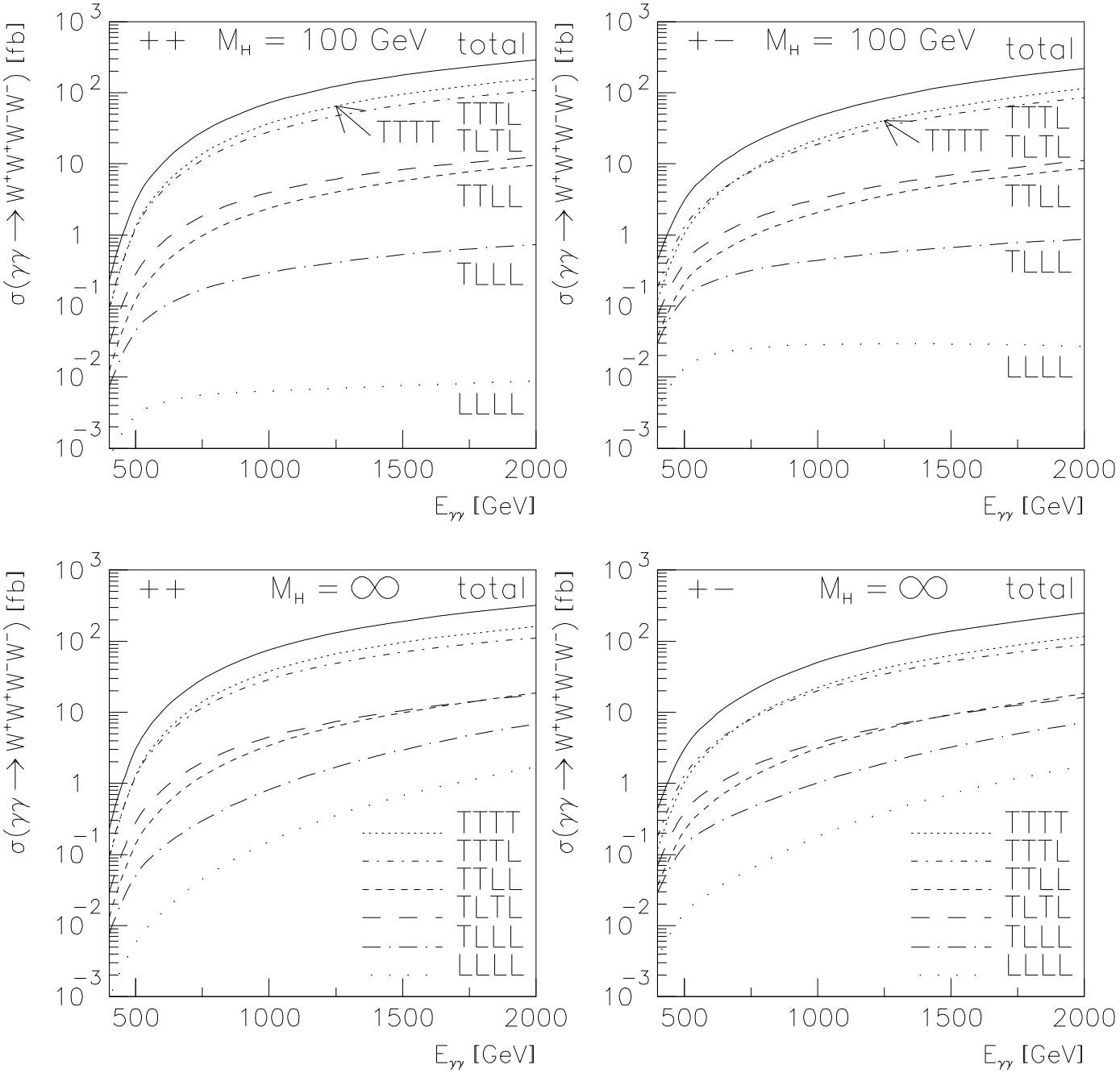

Figure 3. G. Jikia: Four weak boson production ...

This figure "fig1-4.png" is available in "png" format from:

http://arXiv.org/ps/hep-ph/9406395v1

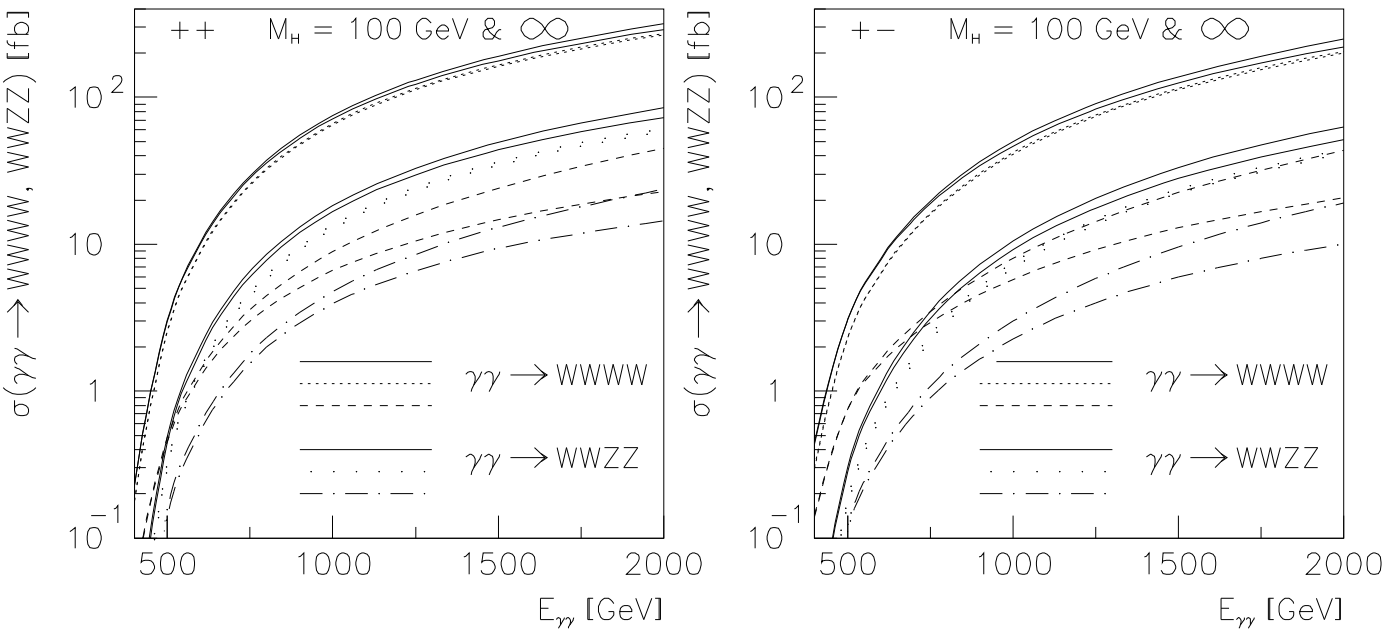

Figure 4. G. Jikia: Four weak boson production ...

This figure "fig1-5.png" is available in "png" format from:

http://arXiv.org/ps/hep-ph/9406395v1

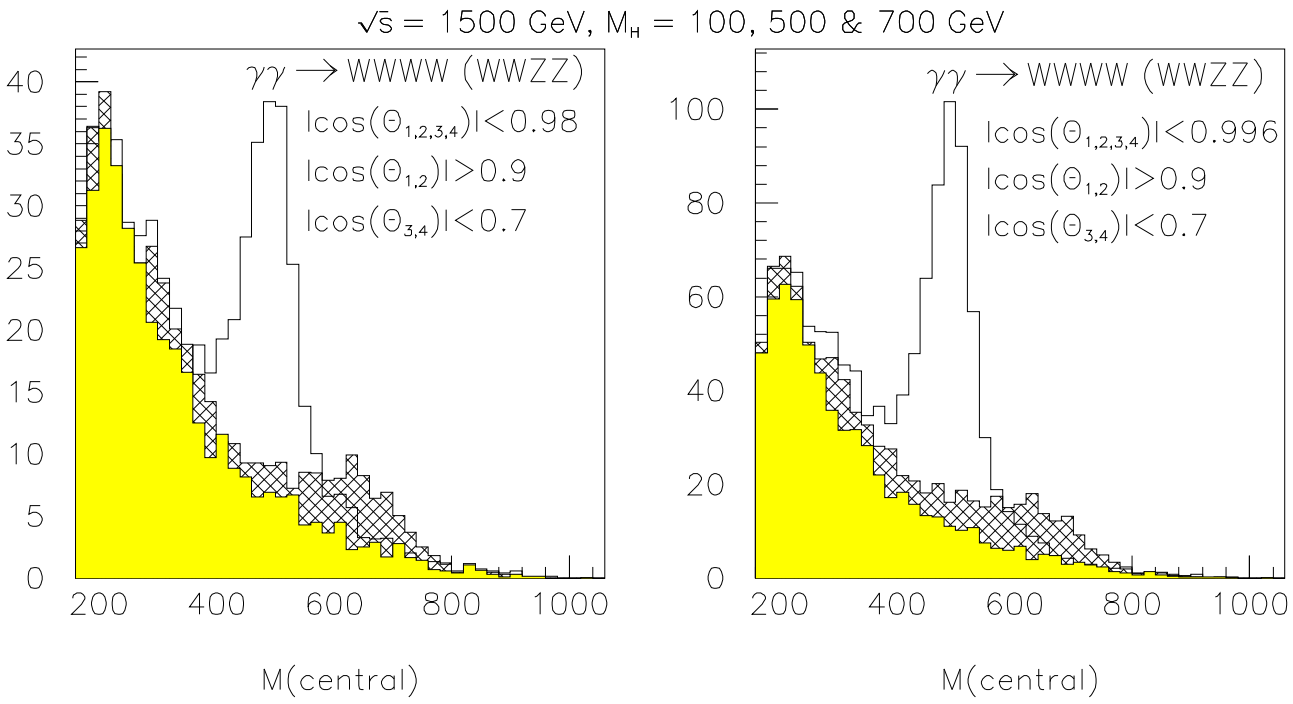

Figure 5. G. Jikia: Four weak boson production ...

This figure "fig1-6.png" is available in "png" format from:

http://arXiv.org/ps/hep-ph/9406395v1

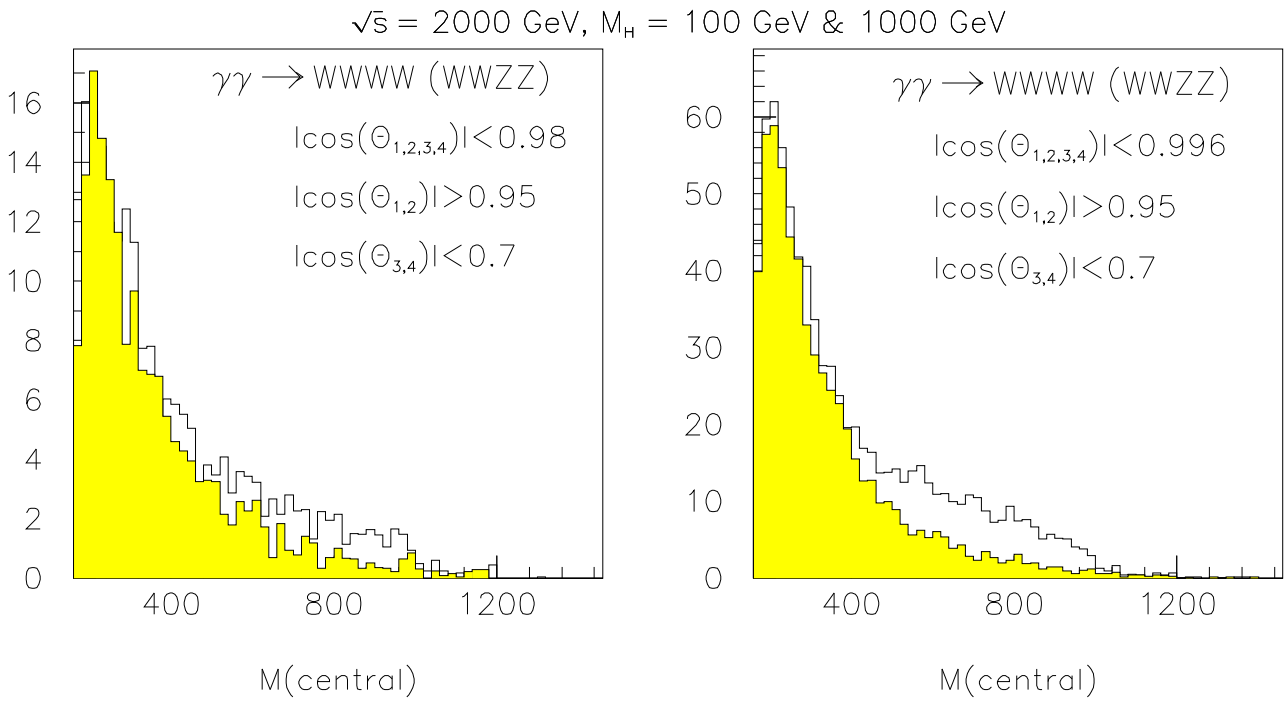

Figure 6. G. Jikia: Four weak boson production ...